

**SUPPLEMENTARY MATERIAL**

**A NEW CATALYTIC MECHANISM OF BACTERIAL FERREDOXIN-NADP<sup>+</sup>  
REDUCTASES DUE TO A PARTICULAR NADP<sup>+</sup> BINDING MODE.**

Paula Monchetti, Arleth S. López Rivero, Eduardo A. Ceccarelli and Daniela L. Catalano-  
Dupuy

**Table S1.** Determination of the content of NADP<sup>+</sup> bound to purified FNR enzymes from different organisms by HPLC.

| <b>Enzyme</b> | <b>NADP<sup>+</sup>/FNR (mol/mol)</b> |
|---------------|---------------------------------------|
| EcFPR         | 0.85 ± 0.15                           |
| PcFPR         | 0.58 ± 0.11                           |
| BaFPR         | 0.30 ± 0.03                           |
| LepFNR        | 0.17 ± 0.01                           |
| PeaFNR        | 0.11 ± 0.03                           |

C18 column with a mobile phase composed of 0.2 M ammonium phosphate, pH 5.1 and a gradient with methanol at a final concentration of 30%. Values are mean ± S.D. of at least three independent measurements.

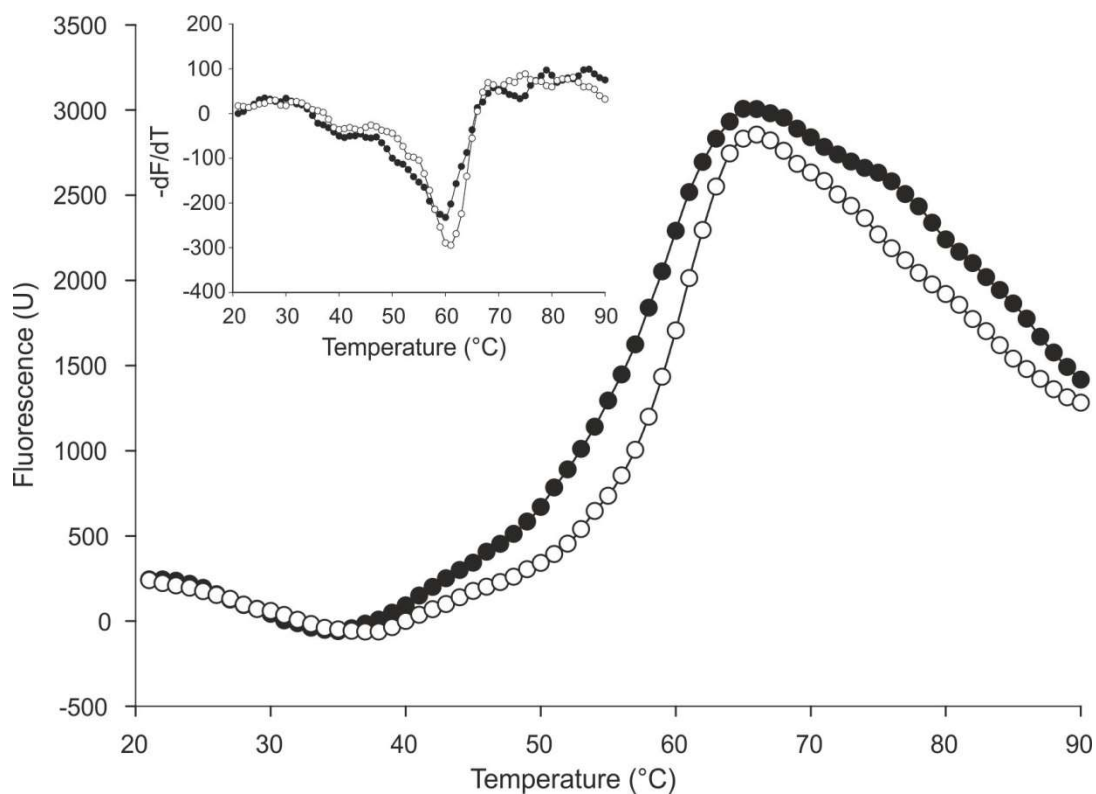


**Figure S1:** Thermal stability of EcFPR\* in the presence or absence of NADP<sup>+</sup>. The fluorescence emitted was plotted as a function of temperature. The inner graph shows the first derivative of fluorescence emission ( $-dF / dT$ ) as a function of the temperature, where the minimum value of the curve corresponds to  $T_m$ . \*EcFPR eluted from the Cibacron Blue column.

**Table S2.** Melting points of thermal unfolding transitions of the FNRs.

| Enzyme | $T_m$ (°C)     |                |
|--------|----------------|----------------|
|        | FNR            | FNR*           |
| EcFPR  | $57.4 \pm 0.7$ | $55.3 \pm 0.9$ |
| PcFPR  | $54 \pm 1$     | $52.5 \pm 0.7$ |
| BaFPR  | $57.6 \pm 0.8$ | $58 \pm 1$     |
| LepFNR | $60 \pm 1$     | $59.4 \pm 0.6$ |
| PeaFNR | $62.3 \pm 0.7$ | $61 \pm 1$     |

Values are mean  $\pm$  S.D. of at least three independent measurements. \*FNR eluted from the Cibacron Blue column.

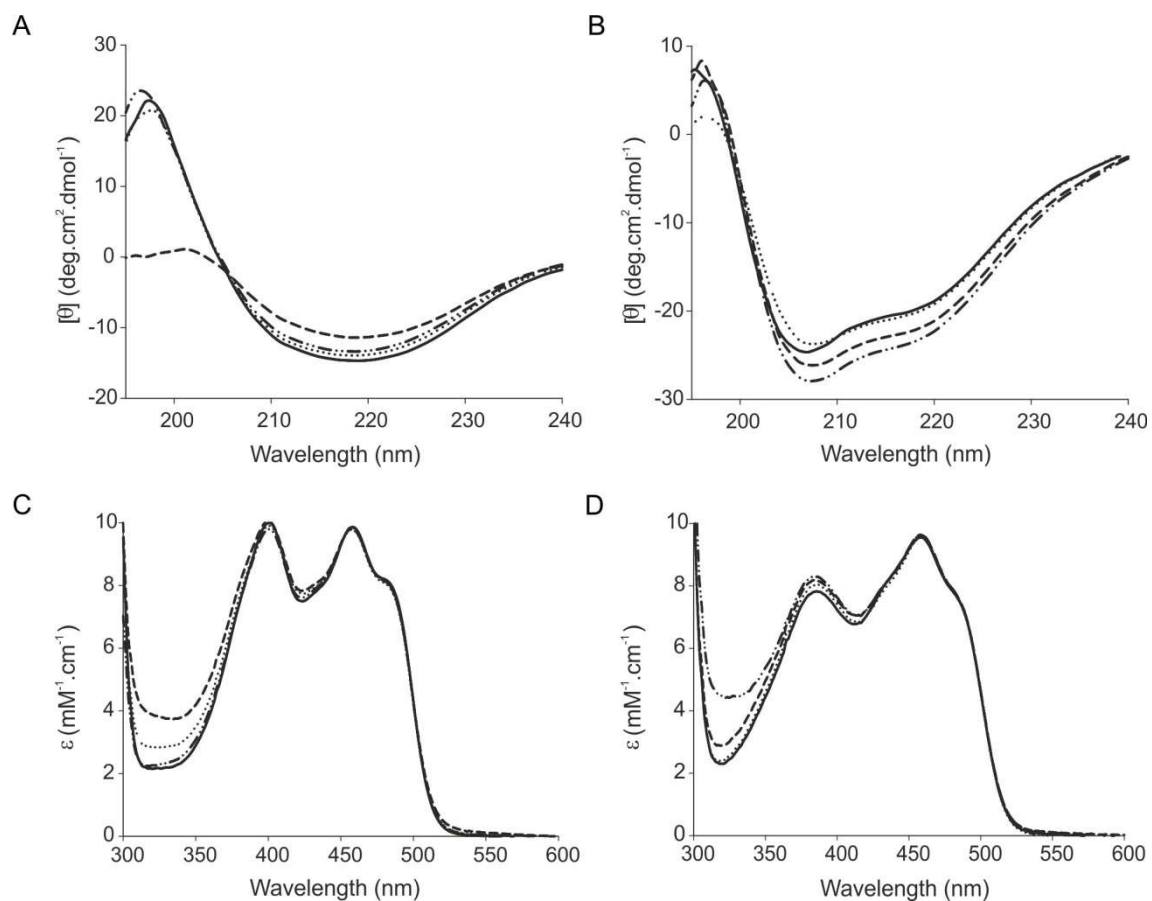


**Figure S2:** Spectroscopic characterization of wild type and mutant EcFPR and PeaFNR. A) and B) Circular dichroism (CD) spectra in the far UV region of EcFPR and PeaFNR, respectively. C) and D) Absorption spectra of EcFPR and PeaFNR, respectively. . Solid line, wild type EcFPR and PeaFNR; dotted line, EcFPR\_R144P and PeaFNR\_P199R; dash line, EcFPR\_R184Y and PeaFNR\_Y240R; dash and dots line, EcFPR\_R144P\_R184Y and PeaFNR\_P199R\_Y240R.

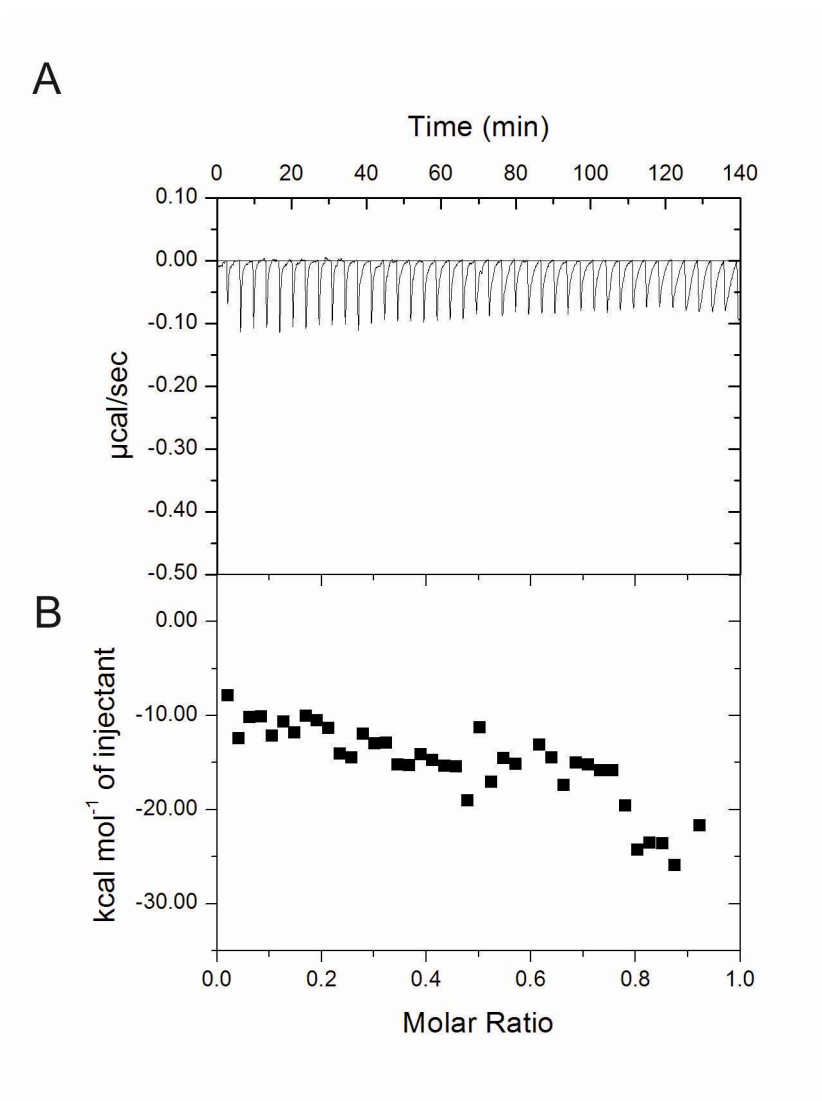


**Figure S3:** Isothermal titration calorimetry (ITC) for the binding of NADP<sup>+</sup> to EcFPR. A) Primary raw data. B) Binding curve derived from the raw data. All the NADP<sup>+</sup> added in substoichiometric quantities formed a complex, showing a constant thermal evolution consistent with the addition of NADP<sup>+</sup>.

**Table S3.** Melting points of thermal unfolding transitions of wild type and mutant EcFPR and PeaFNR.

| Enzyme            | T <sub>m</sub> (°C) |            |
|-------------------|---------------------|------------|
|                   | FNR                 | FNR*       |
| EcFPR             | 58.1 ± 0.6          | 55.3 ± 0.9 |
| EcFPR_R144P       | 59 ± 1              | 59.8 ± 0.8 |
| EcFPR_R184Y       | 57.6 ± 0.6          | 58.2 ± 0.7 |
| EcFPR_R144P_R184Y | 59.4 ± 0.8          | 59.7 ± 0.6 |
| PeaFNR            | 60.3 ± 0.8          | 60.7 ± 0.8 |
| PeaFNR_P199R      | 58.2 ± 0.4          | 58.7 ± 0.6 |
| PeaFNR_Y240R      | 58 ± 1              | 58.5 ± 0.4 |
| PeaFNR_P199_Y240R | 57 ± 1              | 56.4 ± 0.7 |

Values are mean ± S.D. of at least three independent measurements. \*FNR eluted from the Cibacron Blue column.

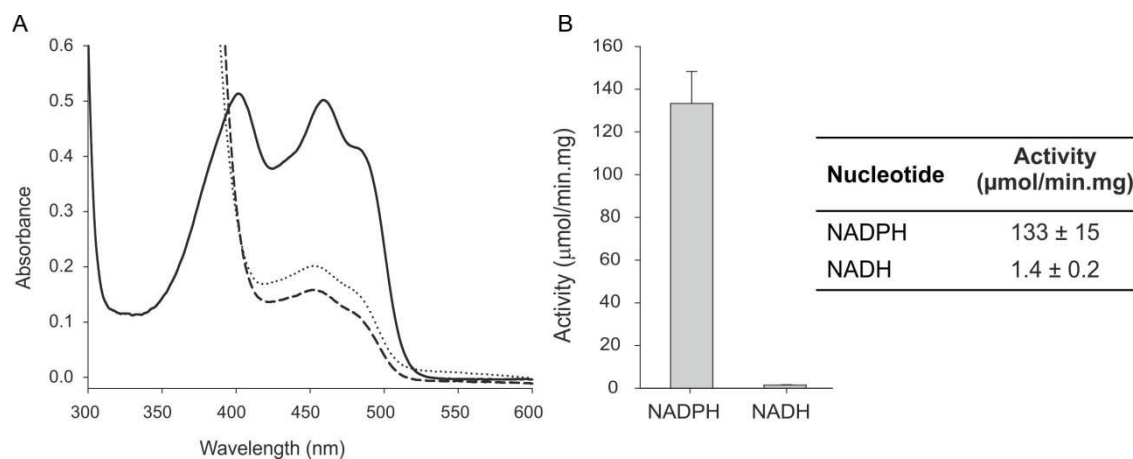


**Figure S4:** Electron transfer between EcFPR and NADPH or NADH. A) Reduction of EcFPR flavin by NADPH or NADH. The spectral changes produced by the addition of the nucleotide substrates are observed in the FAD absorption peak (456 nm). Solid line, EcFPR; dotted line, EcFPR + NADPH; dash line, EcFPR + NADH. B) Determination of NADPH-ferricyanide diaphorase activity of EcFPR.